

Low Temperature Colloidal Synthesis of Silicon Nanorods From Isotetrasilane, Neopentasilane, and Cyclohexasilane

Xiaotang Lu,[†] Kenneth J. Anderson,[§] Philip Boudjouk,[§] and Brian A. Korgel^{†,*}

[†]Department of Chemical Engineering, Texas Materials Institute, Center for Nano- and Molecular Science and Technology, The University of Texas at Austin, Austin, Texas 78712-1062

[§]Center for Nanoscale Science and Engineering, North Dakota State University, Fargo, North Dakota, 58102-5703

*Corresponding author: korgel@che.utexas.edu

Supporting Information

Figure S1 shows the binary phase diagram for Si and Sn. Figures S2-S6 show additional TEM images of Si nanorods made with various polysilicon hydride reactants. Calculation of the Si saturation concentration in a Sn nanoparticle. Calculations of bond dissociation energies for various silanes.

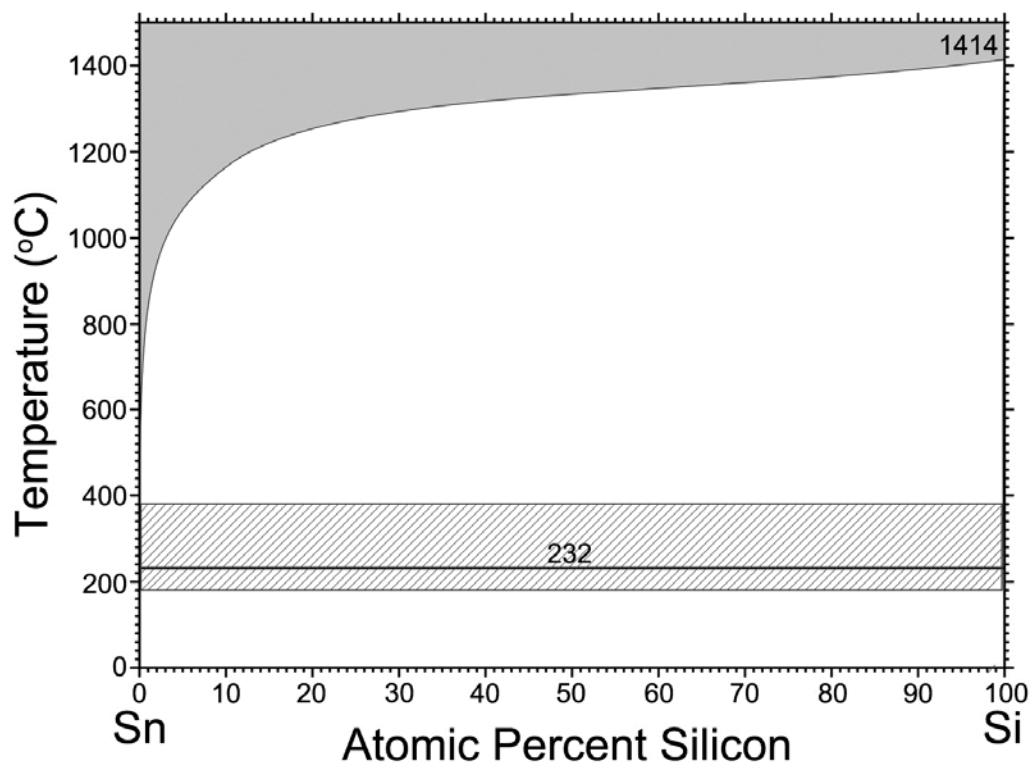


Figure S1. Binary phase diagram of Si-Sn. The eutectic point located at 5×10^{-5} at.% Si and 1×10^{-4} °C is below the melting point of Sn,^{1,2} which cannot be seen in this full composition diagram. The shaded area indicates the temperature range investigated in this work.

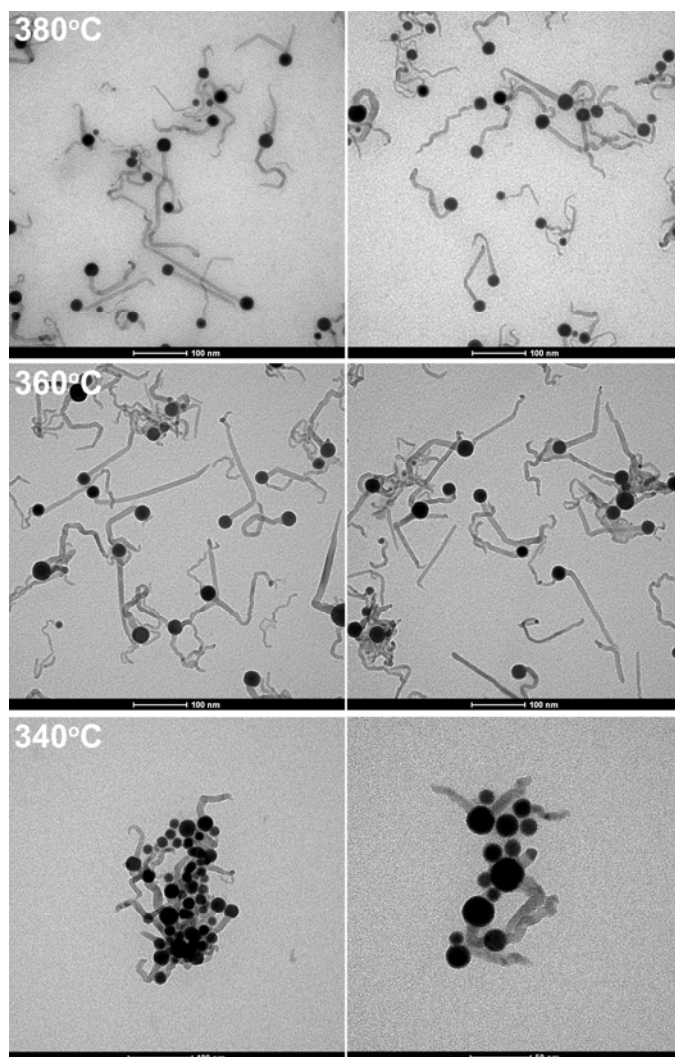


Figure S2. TEM images of the Si nanorods synthesized from trisilane at various temperatures. At 340°C, trisilane exhibits insufficient reactivity that only a few short nanorods were produced.

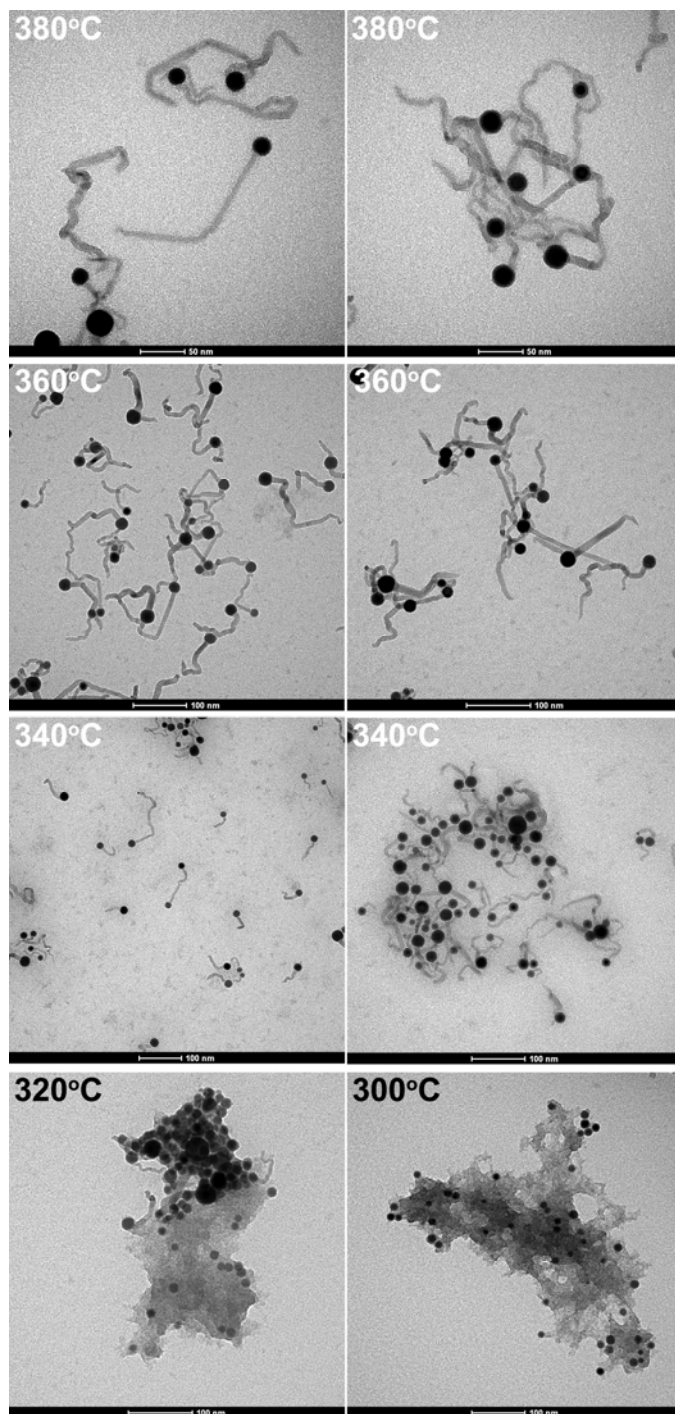


Figure S3. TEM images of the Si nanorods synthesized from isotetrasilane at various temperatures. Isotetrasilane stops to work around 320°C where very few nanorods were produced. At 300°C, the majority of the products become Sn nanoparticles and amorphous Si byproducts.

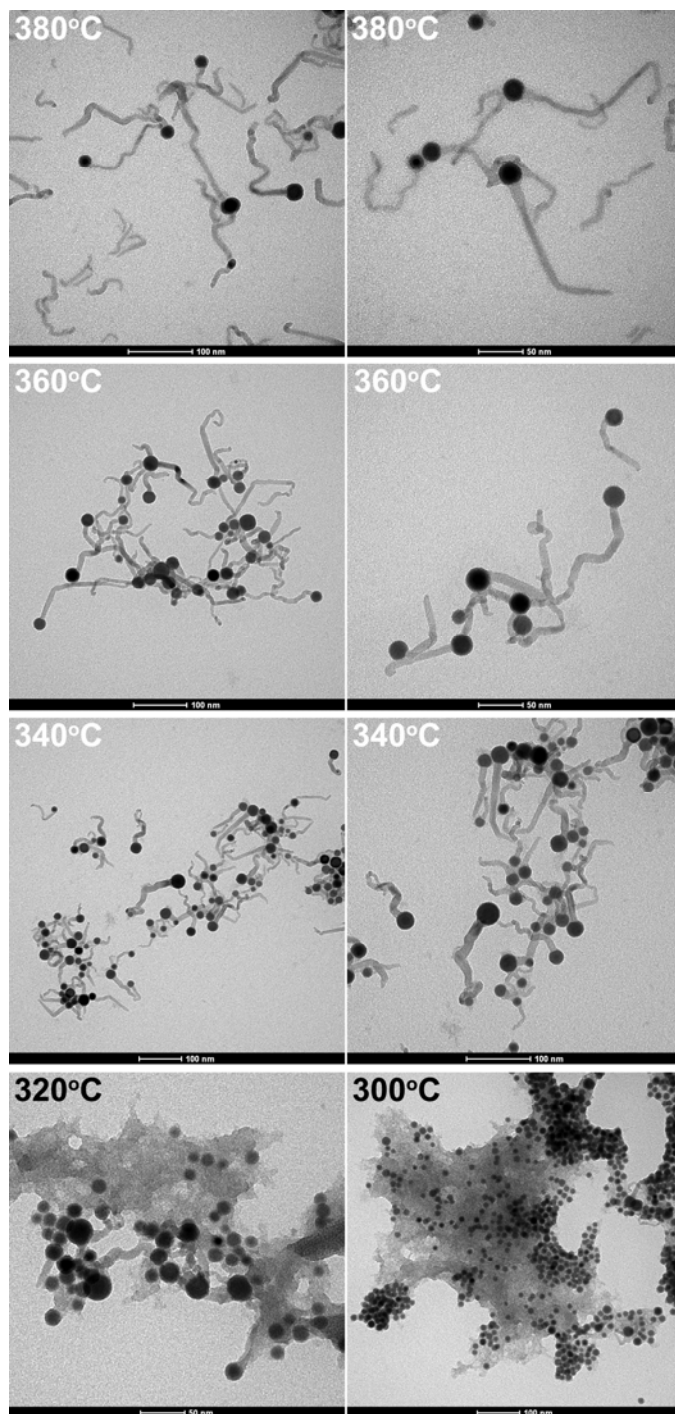


Figure S4. TEM images of the Si nanorods synthesized from neopentasilane at various temperatures. Similar with isotetrasilane, neopentasilane stops to work around 320°C where very few nanorods were produced. At 300°C, the majority of the products become Sn nanoparticles and amorphous Si byproducts.

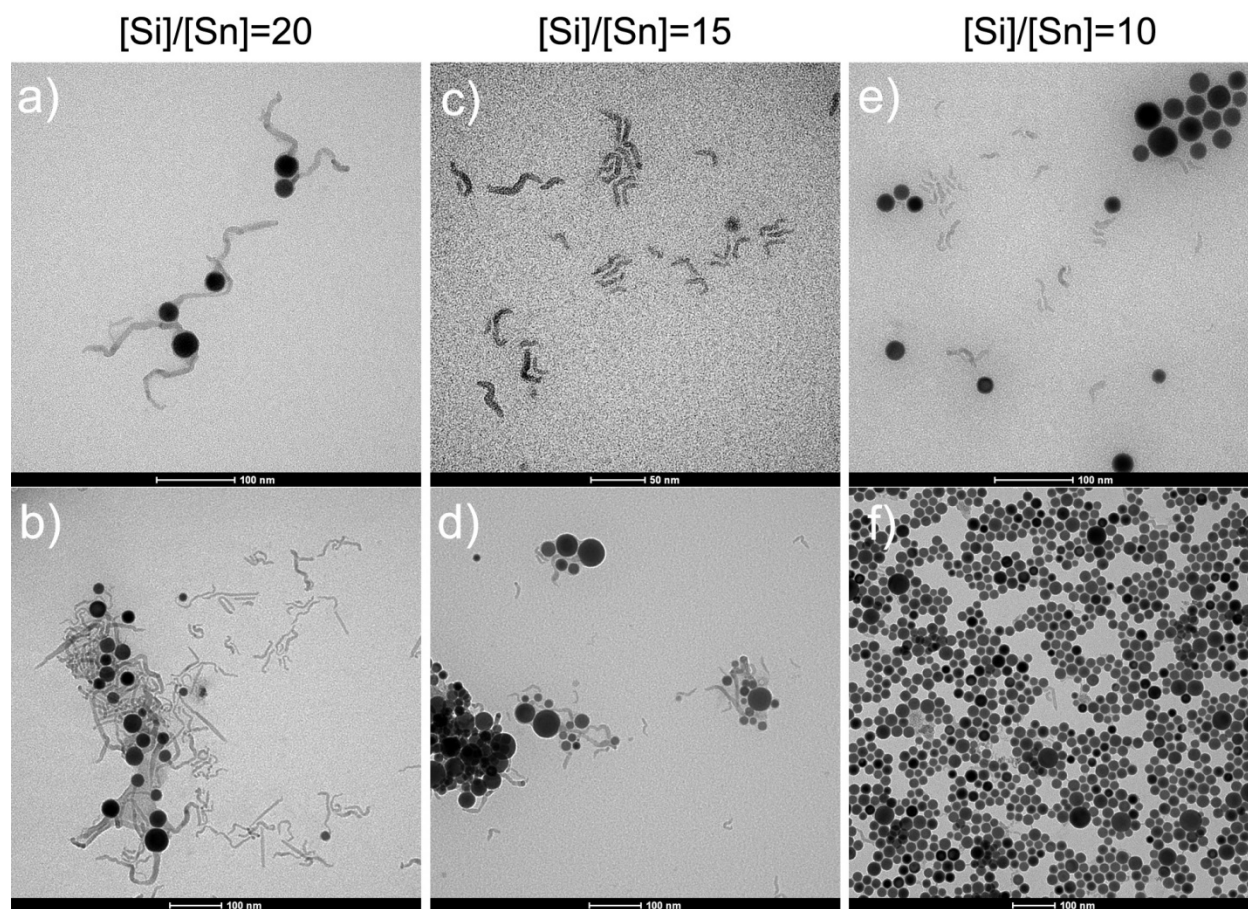


Figure S5. TEM images of products obtained at 380°C with isotetrasilane. (a-b) Long nanorods were obtained with [Si]/[Sn] molar ratio of 20. (c-d) Short nanorods were produced with [Si]/[Sn] molar ratio of 15. (e-f) Only very few short nanorods were obtained with [Si]/[Sn] molar ratio of 10.

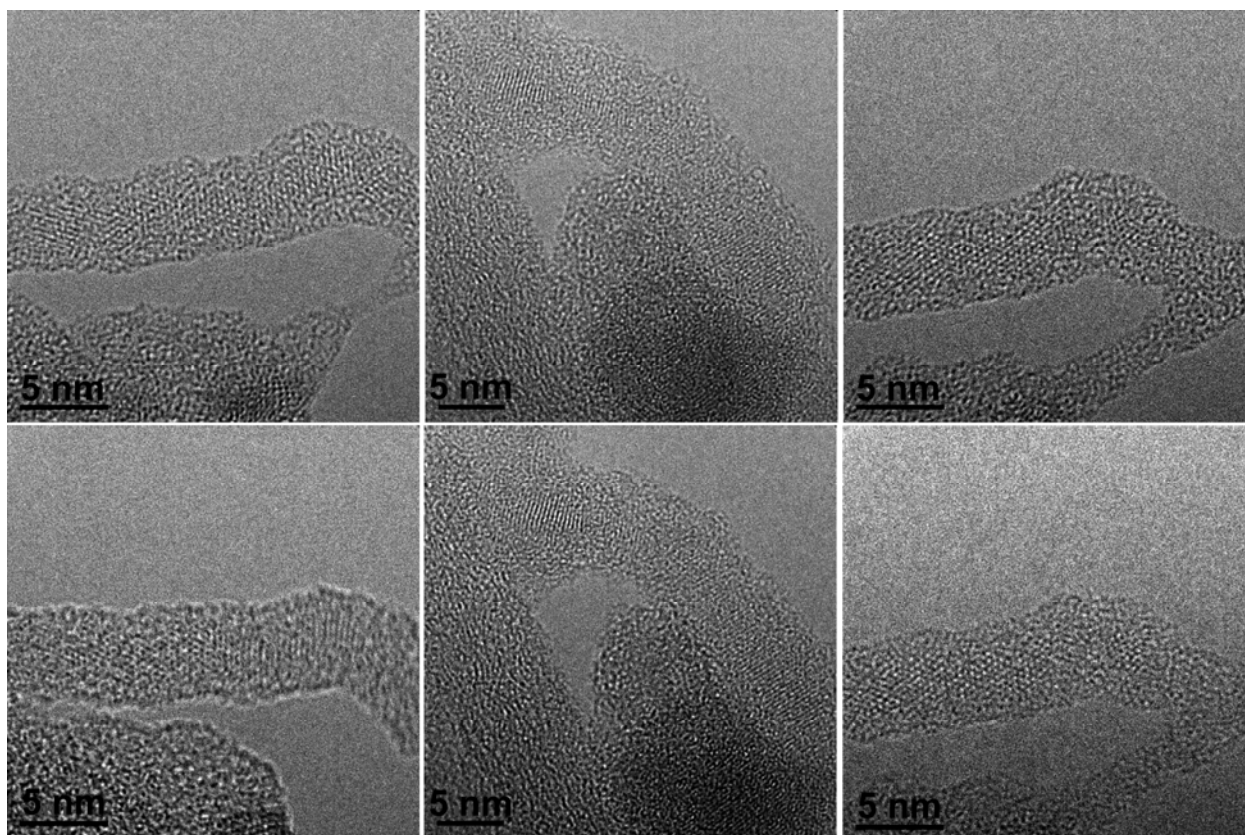


Figure S6. HRTEM images of Si nanorods grown at 200°C with cyclohexasilane. The lattice fringes observed from these nanorods demonstrate that crystalline Si nanorods are still obtained at the relatively low growth temperature. These images were taken with an accelerating voltage of 200 kV on a JEOL 2010F TEM with relatively low beam dose and a limited imaging time of less than 10 min. There was no indication that the beam was affecting the crystallinity of the nanorods and these imaging conditions have been found by others to have no effect on Si crystallinity.^{3,4}

Calculation of Si saturation in a Sn nanoparticle.

For the Sn catalyst nanoparticles of the average diameter of 9 nm,⁵ the number of Sn atoms contained in each nanoparticle is calculated as

density of β -Sn at room temperature, $D = 7.365 \text{ g/cm}^3$

atomic weight of Sn, $M = 118.71$

volume of one Sn nanoparticle, $V = \frac{4}{3} \pi r^3 = 3.82 \times 10^{-19} \text{ cm}^3$

number of Sn atoms in each nanoparticle, $N = \frac{V \cdot D}{M} 6.022 \times 10^{23} \approx 14261$

The solubility of Si in the Sn particle at the growth temperature is determined from the liquidus line of Si-Sn binary phase diagram. From Ref. 2, the equation of the liquidus temperature (T) and the corresponding composition (X_{Si}^1 , on Si portion) is

$$T = \frac{\Delta H_{f,\text{Si}}^0 + a(1 - X_{\text{Si}}^1)^2}{\Delta S_{f,\text{Si}}^0 - R \ln X_{\text{Si}}^1 + b(1 - X_{\text{Si}}^1)^2}$$

where $\Delta H_{f,\text{Si}}^0$ is the change in the enthalpy of fusion of silicon, $\Delta S_{f,\text{Si}}^0$ is the entropy of fusion, a and b are constants independent of temperature and composition and could be obtained from experimental data. For calculation, $\Delta H_{f,\text{Si}}^0 = 50654.3 \text{ J/mol}$, $\Delta S_{f,\text{Si}}^0 = 30.026 \text{ J/mol} \cdot \text{K}$, $a = 31162 \text{ J/mol}$ and $b = 4.03 \text{ J/mol} \cdot \text{K}$ in Si-Sn system.⁶

At the growth temperature of 380°C (653K), X_{Si}^1 is obtained as 1.71×10^{-5} from the equation. This means that 8.4 nm diameter Sn nanoparticles are saturated with only $14261 \times 1.71 \times 10^{-5} \approx 0.24$ silicon atoms.

Bond dissociation energies (BDE) of silicon hydrides.

Table S2. Si-H bond dissociation energy and substituent effect.⁷ (kcal/mol)

bond	SiH ₃ -H	H ₃ SiSiH ₂ -H	(H ₃ Si) ₂ SiH-H	(H ₃ Si) ₃ Si-H
BDE	89.7	86.9	84.2	82.1
ΔBDE	0	-2.8	-5.5	-7.6

Table S3. Some Si-Si bond dissociation energy.⁸ (kcal/mol)

bond	SiH ₃ -SiH ₃	Si ₂ H ₅ -SiH ₃	Si ₂ H ₅ -Si ₂ H ₅
BDE	74	71	68

As the inductive effect decreases rapidly over distance, only neighboring substituent is considered in the calculation, e.g. Si-H BDE of (H₃Si)₂SiHSiH₂-H is treated as same as H₃SiSiH₂-H.

Take isotetrasilane as an example,

$$\text{total Si-H BDE} = 89.7 \times 10 = 897 \text{ kcal/mol}$$

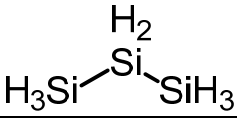
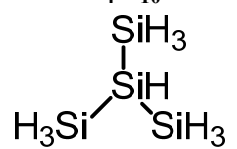
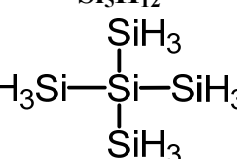
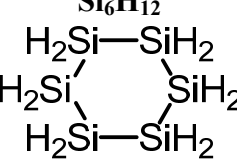
considering substituent effect of silyl radicals,

$$\text{Si-H BDE} = 897 - 7.6 - 2.8 \times 9 = 864.2 \text{ kcal/mol}$$

adding the Si-Si BDE,

$$\text{Si-H \& Si-Si BDE} = 864.2 + 71 \times 3 = 1077.2 \text{ kcal/mol}$$

Table S4. Summary of calculated bond dissociation energies of various silanes (in units of kcal/mol).

Silane	Si-H BDE	Si-H & Si-Si BDE	Si-H BDE per Si	Si-H & Si-Si BDE per Si
Si_3H_8 	689.8	831.8	229.9	277.3
Si_4H_{10} 	864.2	1077.2	216.1	269.3
Si_5H_{12} 	1042.8	1326.8	208.6	265.4
Si_6H_{12} 	1010.4	1418.4	168.4	236.4

References

- (1) Olesinski, R.; Abbaschian, G. The Si-Sn (Silicon-Tin) System. *Bull. Alloy Phase Diagrams* **1984**, *5*, 273–276.
- (2) Bogart, T. D.; Lu, X.; Korgel, B. A. Precision Synthesis of Silicon Nanowires with Crystalline Core and Amorphous Shell. *Dalton Trans.* **2013**, *42*, 12675–12680.
- (3) Ghassemi, H.; Au, M.; Chen, N.; Heiden, P. A.; Yassar, R. S. In Situ Electrochemical Lithiation/delithiation Observation of Individual Amorphous Si Nanorods. *ACS Nano* **2011**, *5*, 7805–7811.
- (4) Takeda, S.; Yamasaki, J. Amorphization in Silicon by Electron Irradiation. *Phys. Rev. Lett.* **1999**, *83*, 320–323.
- (5) Lu, X.; Korgel, B. A. A Single-Step Reaction for Silicon and Germanium Nanorods. *Chem. Eur. J.* **2014**, *20*, 5874–5879.
- (6) Safarian, J.; Kolbeinsen, L.; Tangstad, M. Liquidus of Silicon Binary Systems. *Metall. Mater. Trans. B* **2011**, *42*, 852–874.
- (7) Wu, Y.-D.; Wong, C.-L. Substituent Effect on the Dissociation Energy of the Si-H Bond: A Density Functional Study. *J. Org. Chem.* **1995**, *60*, 821–828.
- (8) Walsh, R. Bond Dissociation Energy Values in Silicon-Containing Compounds and Some of Their Implications. *Acc. Chem. Res.* **1981**, *14*, 246–252.